



Analysis of the Promoting Role of Digital Technology in Innovative Models of Landscape Design

Yanfeng Dong¹, Mengmeng Li² and Chuan Zhao^{1,*}

¹ College of Art, Hebei University of Science and Technology, Shijiazhuang 050000, Hebei, China

² College of Art, Anhui University, Hefei 230601, Anhui, China

SUMMARY: *The present study endeavors to delve into the integration of advanced digital artificial intelligence methodologies within the realm of landscape design. By employing a hybrid approach utilizing convolutional neural networks (CNNs) in conjunction with long short-term memory (LSTM) networks, we aim to scrutinize the intricate relationship between landscape configurations and their influence on vegetation-based carbon sequestration. The ultimate objective is to furnish evidence-based insights that can inform and optimize the strategic planning of urban landscapes. This article uses the CNN-LSTM model to conduct in-depth research on the landscape pattern of regional carbon sequestration land from two scales: landscape and type, and from four levels: morphology, composition, distribution, and structure. Using remote sensing image data, through preprocessing steps such as geometric correction and image dehazing, the landscape pattern index is extracted to explore the relationship between landscape pattern and vegetation carbon sequestration. Research has found that the ED, LSI, IJI, SHEI, AI indices at the landscape scale, as well as the correlation indices of cultivated land, forest land, and grassland at the type scale, are significantly correlated with vegetation carbon sequestration. The impact weights of landscape form, composition, distribution, and structure on vegetation carbon sequestration are 58.69%, 15.79%, 19.36%, and 2.83%, respectively. The application of digital artificial intelligence technology in landscape design helps to enhance the creative, planning, and integration capabilities of landscape architecture, creating practical, aesthetically pleasing, and entertaining landscapes. By optimizing the landscape pattern, especially in terms of form, composition, and distribution, the carbon sequestration effect of vegetation can be effectively improved, promoting the protection of urban ecological environment.*

KEYWORDS: *digitalization; artificial intelligence; Landscape; Vegetation carbon sequestration; Landscape pattern; ecological environment*

1 Introduction

Whether in the past or present, several public health and environmental events in history have prompted urban designers at that time to rethink the relationship between cities and nature, and to consider the importance of outdoor public spaces for densely populated metropolises. The COVID-19 has also sounded an alarm for mankind. The sudden epidemic has made people realize the convenience of the digital era, and people increasingly need digital media, online platforms and virtual technology [1, 2]. With the support of the 5G era and the era of artificial

*A17604662956@163.com

<https://doi.org/10.65102/is20261172>

intelligence, virtual reality technology and other digital technologies have been widely applied in the field of art. Therefore, combining digital artificial intelligence technology with landscape design content, through interdisciplinary research and integration, innovating and transforming the concepts, elements, and techniques of landscape design through artificial intelligence technology, using more three-dimensional, interactive, and participatory methods to design landscape designs that are rich in contemporary characteristics and humanistic spirit [3].

The shaping of urban space by digital artificial intelligence technology affects the development and transformation of urban landscape environment. The cross-border cooperation between digital artificial intelligence technology and landscape design, utilizing and achieving each other, has become a beautiful scenery line that enriches urban landscape. Utilizing information technology to enhance the creative, planning, and integration capabilities of landscape design, creating practical, aesthetically pleasing, and entertaining landscape content [4, 5]. It is a good way to solve the lack of charm in contemporary urban landscape design. Designers can use digital artificial intelligence technology to more intuitively showcase the interactivity, fun, and practicality of garden landscapes, attracting people to participate. At the same time, they can also create unique images and landmarks for different cities, avoiding homogeneity and establishing new urban landmarks. The incorporation of digital artificial intelligence (AI) innovations transcends the traditional boundaries of time, space, the tangible, and the digital, thereby unveiling novel dimensions of urban landscapes for public appreciation. Simultaneously, this integration fosters a heightened level of diversity within landscape design practices. By leveraging digital AI technologies, including sophisticated digital lighting systems and laser projection techniques, in architectural and landscape design endeavors, there is a notable enhancement in energy efficiency. This improvement acts as a mitigating factor against the rapid depletion of environmental resources, thereby indirectly bolstering the preservation of urban ecological systems. Digital AI technology has revolutionized landscape design, transitioning it from a static form to a dynamic, ever-evolving entity. This transformation has given rise to captivating interactive spaces that encourage public engagement, all while maintaining a harmonious balance between the artistic visual representation and the functional aspects of landscape design. Consequently, this synergy significantly elevates the allure and appeal of urban landscape design, making it more engaging and immersive for the urban populace [6].

With the development of technology, digital artificial intelligence technology is gradually being applied in domestic landscape design to express landscape elements. However, at present, it is not deep and extensive enough, so we need to conduct more in-depth exploration and research. This article uses the CNN-LSTM model to explore the impact and spatial differences of the landscape pattern of regional carbon sequestration land on vegetation carbon sequestration from two scales: landscape and type, and four levels: morphology, composition, distribution, and structure. Based on this, taking a certain region as an example, the carbon sequestration effects of different landscape pattern schemes in the region were predicted and compared, which has guiding significance for regional landscape design. The future urban landscape environment will be a landscape space created using digital artificial intelligence technology, breaking the limitations of time and space. Through digital artificial intelligence technology, changes in the spatial environment will be achieved, allowing people living in it to have real-time thinking and sensory interaction. In such a smart, shared, and warm urban landscape environment, residents, tourists, and ourselves will all communicate with each other in a friendly and effective way, jointly realizing the pursuit of a better life.

2 Related research

2.1 GIS Application and Landscape Database Construction

Kunming City launched the "Digital Landscape" project in 1996, utilizing spatial database technologies such as GIS, RS, GPS, computer and network technologies to establish a landscape greening database. Wuhan city has established a garden geographic information system using data collection and database construction technology [7]. Yu Liuqi elaborated on four aspects: green line planning, garden planning, garden green space maintenance and management, and administrative law enforcement work. Reference [8] discussed the research progress on the application of GIS in landscape design at home and abroad, and found that related research in this field is mainly concentrated in developed countries in Europe and America, with most focusing on landscape pattern analysis, biodiversity, land suitability, information management systems, 3D landscape, and landscape sensitivity. Taking the design of plant landscape in residential areas in East China as an example, reference [9] analyzed the functional requirements of landscape space, applied software simulation, and designed a quantified and solidified plant matching module to assemble and assemble residential plant landscape. The study proposed a modular design process and method for plant landscape, which can test and guide the scientific, rational, and diverse layout of plant landscape design. Reference [10] used Java network technology and MySQL database to establish a digital information management system for landscape plants in Shanxi Province, recording 412 species of landscape plants belonging to 193 genera in 102 families. Each plant has a comprehensive graphic and textual page description, which can quickly browse landscape plant information and quickly query and locate plant image information, providing a convenient and practical efficient information platform for landscape designers and related course teaching.

2.2 Landscape Design Methods

Digital artificial intelligence landscape design is the mainstream direction of future landscape design, an important component of urban landscape construction and a reflection of sustainable development, with aesthetic and ecological attributes. Reference [11] discusses the digital technology-based urban green space planning and design methods, elucidates the application of low impact development green space planning methods, and provides useful references for scientific planning research of urban green spaces. Taking the landscape architecture of the Beijing Forestry University Research Center as an example, reference [12] discusses the basic principles, specific applications, and practical experience of digital technologies such as structural finite element analysis, fluid analysis, and sensor driven dynamic landscape architecture. Reference [13] applied digital media to park design, studied the equipment, construction, and demand issues that need to be addressed, and proposed a scientifically reasonable design method, providing ideas and methodological guidance for the design of interactive digital media parks. Reference [14] comprehensively applied information collection technology, data computing platform, mathematical statistics methods, and spatial simulation construction technology to explore the path of refined design of landscape space, and verified its feasibility and operability. The application of digital media technology in ancient architectural landscape design also has significant advantages, which can greatly reduce the workload of designers, improve their work efficiency and creativity. Reference [15] conducted an in-depth study on the application mechanism of digital media technology in vertical design of landscape architecture, detailing various mathematical media art forms such as virtual reality, scene interaction, and landscape modeling. It has important promotion and guidance value for

the development of China's landscape design industry and education and teaching. Reference [16] proposed a large-scale forest scene rendering technique based on OSG (Open Scene Graph), which can draw real-time 3D forest scenes using actual forest survey data, meeting the real-time interaction needs of users. Using OSG scene graphs to organize and optimize scene data can significantly improve the efficiency of scene coloring and overcome the adverse effects of large amounts of tree scene data in gardens. Digital 3D animation is a special form of design applied in landscape art. When integrated with landscape design, it can significantly promote the development of the landscape design industry and has broad application prospects; But to push the application of digital 3D animation to a higher level, it is necessary to conduct in-depth exploration of digital aesthetics.

2.3 Construction of Landscape Information Model

The Landscape Information Model is a digital artificial intelligence model created for the management and optimization of the entire process of "design build operation" in landscape engineering projects. It is an application of BIM (Building Information Modeling) technology for landscape conditions and landscape elements, which can objectively solve the problem of inefficient information exchange in landscape planning projects. Reference [17] applied software such as InfraWorks and Autodesk Civil 3D to construct a ground digital artificial intelligence model of a wetland park in the coal mining subsidence area of Yuncheng County, Shandong Province, in order to explore the construction technology of landscape information models. The model integrates terrain data from three scales: urban area, county area, and park, simulating the geographical landscape of the wetland park, providing feasibility for the practical application of the LIM digital platform. Jiang Xia's research believes that with the cooperation of GIS technology, big data, Internet of Things, oblique photography and other technologies, the digital landscape information model based on BIM+has comprehensive, collaborative and shared functions, which can efficiently and finely manage landscape design and provide decision-making basis and technical support for managers and designers. Reference [18] combines digital virtual technology with digital artificial intelligence in landscape art design and proposes a three-dimensional landscape model construction scheme. By decomposing three-dimensional color and spatial features, the three-dimensional model of rural landscape is reconstructed, and the reconstruction effect of the model is simulated and analyzed. Reference [19] utilized information technologies such as digital Li Sheng and holographic technology to construct a digital Li Sheng intelligent teaching model for plant landscape design, forming a teaching case of smart garden digital Li Sheng.

3 Data sources and processing

3.1 Data sources

The data in this article mainly includes the remote sensing image dataset of garden landscapes used for training and the multi temporal garden landscape remote sensing image data of the research area used for testing and subsequent analysis.

The landscape remote sensing image dataset used for training is divided into two categories [20], one is the publicly available landscape remote sensing image dataset from the CCF competition; One type is high-definition images downloaded from Google Earth for self-made datasets [20]. To ensure the integrity of the training data and the generalization ability of the trained model, the data used for training should include as comprehensive a scene as possible, and should cover image data from different periods, seasons, and lighting conditions. Therefore,

through research and screening, 30 TIF landscape remote sensing images with a size of 4608×4608 were selected for multiple time periods, two different lighting conditions (cloudy and sunny), and three different scenes (urban, rural, wetland). The bands are RGB channels, the image level is 17, the pixel resolution is 1.03 meters, and the scale (72DPI) is 1:727. The six different scenes are shown in Figure 1.



Figure 1: Remote sensing images of garden landscapes in different scenarios

The multi temporal landscape remote sensing images of the research area were obtained from Google Earth historical images. The TIF landscape remote sensing images of the research area were obtained at five different time periods, including February 29, 2014, March 18, 2015, November 11, 2016, June 8, 2017, and May 25, 2024. The images ranged in size from 3000×3000 to 6000×6000 , with three RGB channels and an image level of 17. The pixel resolution was 1.03 meters, and the scale (72DPI) was 1:727.

3.2 Data Processing

In the process of obtaining remote sensing images of garden landscapes, due to the influence of some external comprehensive conditions, such as changes in sensor attitude angles, Earth rotation, terrain undulations, etc., the position and shape of the obtained remote sensing images of garden landscapes may have significant deviations from the corresponding ground features, namely geometric distortions. However, remote sensing data of garden landscapes with significant geometric distortions will have a huge impact on related products of garden landscape remote sensing. Therefore, eliminating geometric distortions has a positive impact on data analysis based on garden landscape remote sensing images [21].

(1) Geometric correction. Although many commercial landscape remote sensing data have undergone basic preprocessing such as geometric correction, there are still some non-systematic random errors between images at different time scales, which result in mismatched target

positions on landscape remote sensing images with different scales but the same location, thereby affecting the results of landscape pattern change analysis. For example, the impact caused by changes in sensor height, posture, etc. This article uses ENVI as a calibration tool and employs a matching method from image to image to register landscape remote sensing images of other time scales with an image of one-time scale as a reference, so that the same geographical coordinates of images of different time scales coincide.

(2) Image dehazing. In addition to geometric deformation, the weather conditions during image capture can also cause significant impacts on subsequent image segmentation processes, such as clouds, fog, and other weather conditions. This study employs a dehazing algorithm grounded in the principle of dark channel precedence, specifically tailored for enhancing images obtained under overcast and fog-laden atmospheric conditions. The concept of the dark channel is delineated as follows:

$$J^{dark}(x) = \min(\min(J^c(y))) \quad (1)$$

Taking pixel point x as the center, take the minimum value within window 2 of each of the three channels, and then take the minimum value of the three channels, which is the dark channel. After obtaining the dark channel, establish an atmospheric physics model as follows:

$$I(x) = A(1-t(x)) + t(x)J(x) \quad (2)$$

where, J is the output image, I is the input cloud and fog weather image, A is the global atmospheric illumination intensity, t is the transmittance, and the process of defogging is the input I and output J . The transmittance formula is as follows:

$$\tilde{t}(x) = 1 - \omega \min_c \left(\min_{y \in \Omega(x)} \left(\frac{I^c(y)}{A^c} \right) \right) \quad (3)$$

where, A^c is the global atmospheric illumination, I^c is the input foggy image, and the formula for atmospheric illumination is as follows:

$$\begin{cases} A^c = [A^R, A^G, A^B] \\ A^R = \text{sum}_R / N \\ A^G = \text{sum}_G / N \\ A^B = \text{sum}_B / N \end{cases} \quad (4)$$

where, sum_R , sum_G , and sum_B respectively add up the coordinates of the brightest pixel point, which is one thousandth of the total number of pixels in the dark channel J^{dark} , at the corresponding points in the three channels (R, G, B) of the original image. Finally, the output dehazing image J is obtained by combining it with the atmospheric physics model, and its formula is as follows:

$$J(x) = \frac{A \max(t(x), t_0) + I(x) - A}{\max(t(x), t_0)} \quad (5)$$

3.3 Landscape Pattern Index

This research endeavors to primarily elucidate the correlation between landscape patterns and

vegetation carbon sequestration. Given that the most recent dataset for vegetation carbon sequestration was recorded in 2017, while the latest land use data pertains to 2024, it was observed that there were minimal alterations in both land use and vegetation carbon sequestration over this one-year interval. To maintain an adequate sample size and ensure the timeliness of our investigation, we have incorporated the 2017 vegetation carbon sequestration data alongside the 2024 land use data to derive the analytical conclusions for the year 2024. In alignment with the research objectives, this study has reclassified land use types into six distinct categories: arable land, forested areas, grasslands, aquatic regions, built-up land, and unutilized land [22].

The Landscape Pattern Index (LPI) stands as a widely adopted quantitative analytical approach within the discipline of landscape ecology, employed to characterize alterations in landscape configuration. This index is structured across three hierarchical tiers: the patch level, the type level, and the landscape level, each offering unique insights into the spatial organization and dynamics of landscapes. Previous studies have shown that landscape patterns of different types and scales have a significant impact on vegetation carbon sequestration. To comprehensively reflect the landscape pattern of the region, this article refers to existing research and selects two scales and nine types of landscape indices to quantitatively characterize its pattern characteristics. The index of landscape scale is used to describe the landscape pattern of mixed-use land, while the index of type scale is used to describe the landscape pattern of single use land such as cultivated land, forest land, and grassland.

The landscape pattern indices chosen for this investigation are delineated as follows, with references to established literature [23]:

1) Patch Density (PD): This metric quantifies the concentration of a specific patch type within the landscape, serving as an indicator of the overall landscape's heterogeneity and fragmentation, as well as the fragmentation extent of a particular patch category.

2) Largest Patch Index (LPI): Employed to identify the prevailing patch type within the landscape architecture, a higher LPI value signifies a greater dominance of that patch type across the landscape.

3) Edge Density (ED): Defined as the total length of edges between patches of dissimilar landscape elements per unit area within the study domain, ED elucidates the degree of landscape fragmentation and edge effects.

4) Landscape Shape Index (LSI): This index gauges the geometric complexity of a patch by comparing its actual perimeter with that of a circle of equivalent area. An elevated LSI denotes a more intricate patch shape.

5) Interspersion and Juxtaposition Index (IJI): A pivotal metric in landscape ecology, IJI characterizes the spatial arrangement of a landscape by assessing the adjacency of a specific patch type to other patch types within the landscape.

6) Division Index (DIVISION): This indicator quantifies the extent of patch isolation in landscape architecture, reflecting both the fragmentation level and spatial intricacy of the landscape.

7) Shannon's Evenness Index (SHEI): SHEI evaluates the evenness of patch type distribution within garden landscapes. A lower SHEI value suggests the dominance of certain patch types, whereas a value approaching 1 indicates a more uniform distribution of patch types, with no single type predominating.

8) Aggregation Index (AI): AI assesses the connectivity among patches of each landscape type. A lower AI value implies a more fragmented landscape, with patches being less interconnected.

4 Landscape pattern prediction based on CNN-LSTM

4.1 CNN Network

The architectural configuration of a Convolutional Neural Network (CNN) typically encompasses convolutional layers, activation functions, pooling layers, fully connected layers, and batch normalization layers. Throughout the training phase, the CNN evaluates the loss function associated with the model's parameters by following the gradient's direction. Subsequently, it updates these parameters in the direction opposite to the gradient, thereby progressively diminishing the loss function's value. This process involves a reverse adjustment of the network weights, with continuous refinement of the network parameters aimed at enhancing the model's accuracy. However, existing CNN based image recognition methods are not suitable for processing temporal data such as landscape remote sensing [24, 25].

One dimensional convolutional neural network (1DCNN) is often used to identify and extract features of time series, and similar to CNN, it also has the advantages of translation invariance, which can effectively extract key features from landscape remote sensing data. Consequently, this research opts for a one-dimensional Convolutional Neural Network (1DCNN) as the framework for processing landscape remote sensing datasets. The 1DCNN architecture comprises three convolutional layers, interspersed with pooling layers and batch normalization (BN) layers, alongside a solitary fully connected layer and a randomly deactivated regularization layer, known as Dropout. The detailed configuration of this model is illustrated in Figure 2.

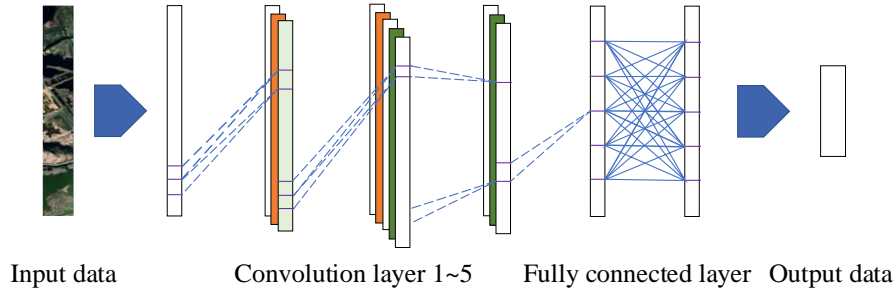


Figure 2: Structure of the 1DCNN Model

The data matrix size of the collected remote sensing raw data of garden landscape after preprocessing and overlapping windows is 6×256 . After data input, perform one-dimensional convolution calculation on its time domain using the following formula:

$$h_j^l = \sum_{i=1}^n x_i^l \otimes k_{ij}^l + b_j^l \quad (6)$$

where, h is the output feature vector; b is the bias vector; x is the input feature vector; l is the number of layers; I is the convolution ordinal number; n is the length of x ; J is the element ordinal number; k is the convolution kernel representing matrix multiplication.

In 1DCNN, the convolutional kernel can be regarded as a receptive field. To reduce computational complexity, the same convolutional kernel shares a set of weights when performing operations on different local data. The calculation formula is:

$$\text{Cov}(x, y) = \sum_{a=0}^{\infty} G(x-a) \times F(a) \quad (7)$$

where, Cov is the output sequence of convolution operation; w is the size of the convolution kernel; $G(x-a)$ is the local vector matrix computed with the convolution kernel function; a is the size of the convolution kernel in the input width direction; $F(a)$ is the convolution kernel parameter vector.

Pooling the output feature map after convolution can reduce the size of the feature map, thereby reducing computational complexity and to some extent preventing overfitting, improving the model's generalization ability. The calculation formula is:

$$P = \max_w \{A^L\} \quad (8)$$

where, P is the feature after maximum pooling; A is the activated feature matrix; W is the width of the pooling area; L is the width of the feature map set.

After each convolutional layer, use a BN layer to prevent model overfitting, and after the BN layer, use a ReLU activation function. It is a nonlinear activation function, which has the advantage of mapping negative values to 0, thereby making the output of some neurons 0, improving the expression ability of the model, reducing redundant information, and alleviating the problem of gradient vanishing. The calculation formula is:

$$\text{ReLU}(x) = \begin{cases} x, & x \geq 0 \\ 0, & x < 0 \end{cases} \quad (9)$$

During the training process, a loss function is introduced to measure the performance of the model and optimize it. This article selects the commonly used cross entropy loss function in deep learning. The calculation formula is:

$$L(\theta) = -\frac{1}{n} \left[\sum_{i=1}^n \sum_{k=1}^K I\{y_i = k\} \lg \frac{\exp(\theta_k^T x)}{\sum_{j=1}^K \exp(\theta_j^T x)} \right] \quad (10)$$

where, $I\{y_i = k\}$ is the indicator function. When the true category y of sample i is equal to category k , the value is 1; otherwise, the value is 0; K is the number of categories; θ is the parameter of the model.

Employ a fully connected layer to transform the output from the preceding layer into a one-dimensional vector, which subsequently serves as the input. This vector is then multiplied by its corresponding weight matrix. To mitigate the risk of model overfitting, a Dropout layer is incorporated immediately following the fully connected layer. While the application of a one-dimensional Convolutional Neural Network (1DCNN) excels in extracting temporal features and is adept at managing tasks involving local information, it exhibits limitations in effectively capturing the global characteristics inherent in landscape remote sensing data. This constraint consequently impacts the overall performance of the model.

4.2 LSTM Network

Long Short-Term Memory (LSTM) networks represent an advanced variant of recurrent neural network (RNN) architectures, specifically engineered to tackle the long-term dependency challenges that plague conventional RNNs. By integrating gating mechanisms, LSTMs achieve superior performance in processing lengthy sequential data, effectively mitigating issues related to vanishing or exploding gradients that often hinder traditional RNNs. The input, output, forget

gates, and memory units make up the majority of LSTM [26, 27].

These three gates all have Sigmoid activation mechanisms. The forget gate regulates whether previously recorded historical knowledge is retained, while the input and output gates respectively control the input and output information of neurons at any given time. Set the hidden layer size to 128 and the learning rate to 0.001. Its structure is shown in Figure 3.

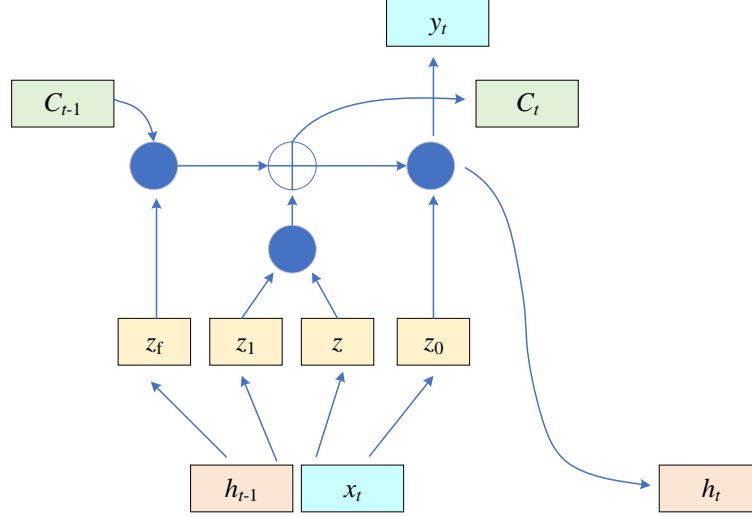


Figure 3: LSTM Unit Structure

The forget gate is used to control the information that can be retained in the current time from the previous unit state, and its calculation formula is:

$$f_t = \sigma(b_f + W_f [h_{t-1}, x_t]) \quad (11)$$

where, W_f is the weight matrix of the forget gate; h_{t-1} is the output from the previous moment; b_f is the bias value of the forget gate; x_t is the input at the current time.

The input gate in a neural network architecture, such as in Long Short-Term Memory (LSTM) units, is tasked with the critical function of deciding whether the current input to the network should be retained within the cell state. This decision-making process is governed by a specific computational formula, which can be mathematically articulated to facilitate the precise control of information flow into the cell state.

$$\begin{cases} i_t = \sigma(b_i + w_i [h_{t-1}, x_t]) \\ \hat{C}_t = \tanh(b_c + W_c [h_{t-1}, x_t]) \\ C_t = i_t \hat{C}_t + f_t C_{t-1} \end{cases} \quad (12)$$

where, w_i is the weight matrix of the input gate; b_i is the bias value of the input gate; \tanh is the activation function.

The output gate controls the output at the current time, combining the previous state with the current input to generate the output at the current time. The calculation formula is:

$$\begin{cases} \sigma_t = \sigma(W_o [h_{t-1}, x_t] + b_o) \\ h_t = o_t \tanh(C_t) \end{cases} \quad (13)$$

where, W_o is the weight matrix of the input gate; b_o is the bias value of the input gate.

As a recurrent neural network suitable for sequential data, LSTM can effectively capture long-term dependencies in time series, providing powerful modeling capabilities. This article investigates how combining LSTM with CNN and CBAM can better capture long-term correlations in sequences when processing data with temporal properties, thereby improving the predictive accuracy of the model.

4.3 CNN-LSTM Network

The advantage of combining convolutional neural networks with temporal deep learning methods is that they can simultaneously capture the temporal and spatial correlations of data. Common convolution kernels (such as $3 \times 35 \times 5$, etc.) and max pooling (such as 2×2) shapes have been widely used in previous studies using CNN-LSTM models. Given the dataset constructed in this article, a one-dimensional convolutional neural network (1D-CNN) structure is used for feature extraction of input data. In the field of landscape design, 1D-CNN has been successfully applied to the problem of landscape pattern prediction. 1D-CNN adopts a one-dimensional convolution and pooling structure, which can selectively extract key features from the constructed dataset.

The CNN section consists of two convolutional layers and one pooling layer. The first convolutional layer uses three 5×1 and six 1×9 convolution kernels, while the pooling layer uses three 3×1 and six 1×3 pooling kernels. The second convolutional layer uses three 3×1 and six 1×3 convolution kernels. Horizontal convolution kernels of 1×3 and 1×9 are used for feature extraction in the horizontal direction. 3×1 and 5×1 vertical convolution kernels are used for feature extraction in the vertical direction. The LSTM part adopts a single LSTM structure containing multiple hidden layers, with 1024 hidden neurons per hidden layer, and finally outputs the prediction results through three fully connected layers. The specific model structure is shown in Figure 4.

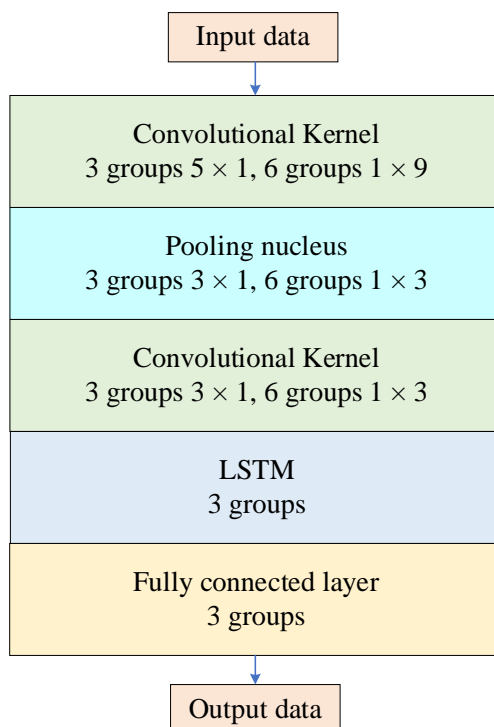


Figure 4: Structure of CNN-LSTM Hybrid Model

5 Empirical analyses

Research data shows that the vegetation carbon sequestration in the studied areas from 2006 to 2024 was 309, 341, 338, 409, and 393 million tons, respectively. The annual average vegetation carbon sequestration in the districts and counties was 2.19, 2.42, 2.40, 2.90, and 2.79 million tons, respectively. It can be seen that before 2016, the growth of vegetation carbon sequestration in the region was relatively slow or even decreased. This is because the early development of urban agglomerations was mainly based on development and construction, and the expansion of construction land brought about a reduction in carbon sink land.

The carbon sequestration land in the region has decreased from 183200 km in 2006 to 17.86k m² in 2024, showing a continuous decreasing trend. Among them, arable land and grassland have slightly decreased, while forest land has increased (Table 1). This is related to China's comprehensive implementation of the Grain for Green project since 2002 and the active response of various regions to the policy requirements of forest reclamation. Compared with the trend of changes in vegetation carbon sequestration, the decrease in carbon sink land area is accompanied by an increase in vegetation carbon sequestration instead of a decrease, indicating that in addition to the scale area, the landscape pattern of carbon sink land also plays an important role in the carbon sequestration effect of vegetation.

Table 1: Changes in Carbon Sequestration Land Use in the Study Areas from 2006 to 2024 (Area/Square Kilometer)

Land use Type	2024 year		2021 year		2016 year		2011 year		2006 year	
	Area	Account	Area	Account	Area	Account	Area	Account	Area	Account
Cultivated land	115922	64.89%	116782	64.94%	117686	65.08%	118182	64.76%	119217	65.08%
Woodland	51987	29.10%	51557	28.67%	51626	28.55%	51036	27.97%	50656	27.65%
Grass	10739	6.01%	11501	6.40%	11529	6.38%	13272	7.27%	13315	7.27%
Total	178649	100%	179840	100%	180840	100%	182490	100%	183188	100%

In order to comprehensively and systematically analyze the carbon sequestration effect of landscape patterns, this paper selects the landscape indices of two scales in Table 2 as influencing factors for research. Using ArcGIS software, the land use data of the study area was split and processed according to the administrative boundaries of each county. The processed land use data of each county was input into Fragstats4.2 software for batch calculation, and various landscape indices of each county were obtained. At this point, if all indices are calculated as input data for the neural network, it will increase the complexity of the network and reduce its performance, even affecting the accuracy of the calculation results. Therefore, before using the CNN-LSTM neural network model, it is necessary to exclude factors with insignificant correlation at the landscape and type levels through correlation analysis.

Table 2: Correlation between Landscape Index and Vegetation Carbon Sequestration at Landscape Scale

Landscape Index	Correlation coefficient				
	2024 year	2015 year	2016 year	2005 year	2006 year
Plaque density (PD)	0.4633	0.3654	0.2915	0.3784	0.3445
Maximum Plaque Index (LPI)	0.0011	0.0076	0.0156	-0.0046	-0.0019
Edge density (ED)	0.4874**	0.5692**	-0.4797**	-0.3409	-0.3425
Landscape Shape Index (LSI)	0.1864*	0.2025 **	0.1746**	0.1483**	0.1397**
Spread and Parallel Index (IJI)	-0.0107	-0.0176*	-0.0138*	-0.0167*	-0.0152*
Landscape Segmentation Index (DIVISION)	0.3369	1.4879	1.9807	-0.3256	-0.0904
Fragrant Uniformity Index (SHEI)	2.7924*	2.6254*	2.7424**	2.8793**	3.3096**
Aggregation Index (AI)	4.7518**	5.2968**	4.4667**	3.3224*	3.2757

Note: * * indicates significant correlation at the 0.01 level; *There is a significant correlation at the 0.05 level.

This article conducts regression analysis between the landscape indices of five different periods and vegetation carbon sequestration, and obtains the analysis results of each landscape index (Table 2). Overall, the R^2 values of the regression model are 0.793, 0.805, 0.864, 0.860, and 0.866, respectively, indicating that the landscape pattern at the landscape level has a significant impact on vegetation carbon sequestration. Among them, the correlation between patch density (PD), maximum patch index (LPI), landscape segmentation index (DIVISION) and vegetation carbon sequestration is not significant. Landscape shape index (LSI), richness uniformity index (SHEI), and aggregation index (AI) are positively correlated with vegetation carbon sequestration, while edge density (ED), dispersion and parallelism index (IJI) are negatively correlated with vegetation carbon sequestration. This indicates that a garden landscape pattern with complex shapes, clustered patches, uniform types, and moderate patches has a better effect on vegetation carbon sequestration. Regression analysis was conducted between the landscape indices of five different time periods and vegetation carbon sequestration (Table 3).

Table 3: Correlation between Type Scale Landscape Index and Vegetation Carbon

Sequestration

Land use type	Landscape Index	Correlation coefficient				
		2024 year	2015 year	2016 year	2005 year	2006 year
Cultivated land	Proportion of Landscape Types (PLAND)	0.0209	0.0274	0.0171	0.0284	0.0164
	Plaques density (PD)	0.9953	0.3276	0.6376	1.3206	0.6453
	Maximum Plaques Index (LPI)	0.0139	0.0167	0.0218	0.0058	0.0038
	Edge density (ED)	-0.0397	-0.0672*	-0.0546*	-0.0549*	-0.0637**
	Landscape Shape Index (LSI)	0.0346*	0.0385*	0.0383*	0.0128	0.0256*
	Spread and Parallel Index (IJI)	-0.0054	-0.0114*	-0.0087	-0.0106	-0.0124
	Landscape Segmentation Index (DIVISION)	1.6787	2.3315	2.6445*	0.9352	0.7975
	Aggregation Index (AI)	-0.1247	-0.2946	-0.1929	-0.3267	-0.2763*
Woodland	Proportion of Landscape Types (PLAND)	0.0836 **	0.0874**	0.0676**	0.0554*	0.0410
	Plaques density (PD)	0.6137	0.4028	0.5475	0.6787	0.3328
	Maximum Plaques Index (LPI)	-0.0148	-0.0236	-0.0146	-0.0006	-0.0046
	Edge density (ED)	-0.2019**	-0.1998**	-0.1657**	-0.1469*	-0.1175**
	Landscape Shape Index (LSI)	0.0835**	0.0826*	0.0636**	0.0647*	0.0487*
	Spread and Parallel Index (IJI)	-0.0127	-0.0120	-0.0139*	0.000	-0.0009
	Landscape Segmentation Index (DIVISION)	1.1954	0.3846	0.0987	1.1306	0.0524
	Aggregation Index (AI)	0.0959*	0.0828*	0.0616	0.0428	0.0215
Grass	Proportion of Landscape Types (PLAND)	0.1787*	0.1664*	0.1552*	0.1546**	0.1346*
	Plaques density (PD)	-1.8993	-1.7327	-2.3907*	-2.2987	-1.9054
	Maximum Plaques Index (LPI)	-0.0975	-0.0609	-0.1282	-0.0396	-0.0203
	Edge density (ED)	-0.0768	-0.0865	-0.0636	-0.1254*	-0.1096**
	Landscape Shape Index (LSI)	0.0187	0.0217	0.0215	0.0468**	0.0375*
	Spread and Parallel Index (IJI)	-0.0025	-0.0024	-0.0017	0.0019	0.0028
	Landscape Segmentation Index (DIVISION)	94.3296*	101.2259*	57.8882	74.0338**	74.8426*
	Aggregation Index (AI)	-0.0045	-0.0076	-0.0018	0.0017	0.0019

Note: ** indicates significant correlation at the 0.01 level; *There is a significant correlation at the 0.05 level.

Compared with the landscape indices of different time periods, the landscape indices of different time periods had a greater impact on vegetation carbon sequestration. The R^2 values of the regression models were 0.918, 0.916, 0.938, 0.934, and 0.936, respectively. Among them, the correlation between PD and LPI indices of cultivated land landscape and vegetation carbon sequestration is not significant, the significance of IJI and DIVISION indices is unstable, LSI index is positively correlated with vegetation carbon sequestration, and ED and AI indices are negatively correlated with vegetation carbon sequestration. This indicates that the more complex the shape of cultivated land, the more regular its edges, and the more dispersed its pattern, the higher its carbon sequestration effect; The correlation between PD, LPI, DIVISION indices of forest landscape and vegetation carbon sequestration is not significant, while the significance of IJI and AI indices is unstable. LSI index is positively correlated with vegetation carbon sequestration, while ED index is negatively correlated. This indicates that the higher the

proportion of forest land, the more complex its shape, and the more regular its boundaries, the higher the carbon sequestration effect of vegetation; The correlation between LPI, IJI, AI indices of grassland landscape and vegetation carbon sequestration is not significant, the significance of PD index is unstable, LSI and DIVISION indices are positively correlated with vegetation carbon sequestration, and ED index is negatively correlated with vegetation carbon sequestration. This indicates that the higher the proportion of grassland, the more complex its shape and structure, and the more regular its boundaries, the higher the carbon sequestration effect of vegetation.

In summary, a total of 15 landscape indices, including ED, LSI, IJI, SHEI, and AI indices at the garden landscape scale, ED, LSI, and AI indices for cultivated land at the type scale, ED, LSI indices for forest land, and ED, LSI, and DIVISION indices for grassland, are significantly correlated with vegetation carbon sequestration. According to the ecological significance of various landscape indices, the influencing factors of landscape pattern on vegetation carbon sequestration can be summarized into four types: morphology, composition, distribution, and structure (Table 4).

Table 4: Classification of Factors Influencing Landscape Patterns Significantly Related to Vegetation Carbon Sequestration

Landscape pattern of gardens	Landscape Scale of Landscape Architecture	Landscape Index
Landscape form of gardens	landscape architecture	Edge Density (ED) (Negative Correlation), Landscape Shape Index (LSI)
	Type	Farmland edge density (EDe) (negative correlation), forest edge density (EDI) (negative correlation), grassland edge density (EDg) (negative correlation)
		Farmland Landscape Shape Index (LSI), Forest Landscape Shape Index (LSI), Grassland Landscape Shape Index (ISIg)
Composition of Landscape Architecture	Landscape architecture	Spread and Parallel Index (IJI) (Negative Correlation)
	Type	Proportion of Forest Landscape Types (PLANDI) and Grassland Landscape Types (PLANDg)
Landscape distribution in gardens	Landscape architecture	Aggregation Index (AI)
	Type	Arable Land Agglomeration Index (AIe) (Negative Correlation)
Landscape Architecture Structure	Landscape architecture	Fragrant Uniformity Index (SHE)
	Type	Grassland Landscape Segmentation Index (DIVISIONg)

According to the results of neural network calculations, the weights of the impact of landscape form, composition, distribution, and structure on vegetation carbon sequestration are 58.69%, 15.79%, 19.36%, and 2.83%, respectively. This indicates that the landscape form of carbon sink land has the greatest impact on vegetation carbon sequestration, while the composition and distribution of landscape have a greater impact, and the structure has the smallest impact. Therefore, in the planning and design of landscape patterns, in order to enhance the carbon sequestration effect, it is necessary to focus on strengthening the research on the form, composition, and distribution of landscape patterns of carbon sequestration land. Among

them, for the landscape form, the edge density (ED) can be reduced by moderately merging fragmented small patches, and the landscape shape index (LSI) can be improved by designing complex forms of cultivated land, forest land, and grassland landscapes; For the composition of garden landscapes, patches of the same type can be concentrated into patches to reduce the dispersion and parallel index (IJI) of various garden landscapes, and the proportion of forest land and grassland can be increased as much as possible when conditions permit; For the distribution of garden landscapes, forests and grasslands can be moderately connected, farmland can be moderately dispersed, and the aggregation and connectivity (AI) of carbon sequestration land can be adjusted in a differentiated manner, ultimately achieving the effect of improving carbon sequestration.

6 Conclusion

In response to the problems of time-consuming and inefficient data processing tasks in traditional landscape pattern analysis, this paper focuses on pixel level semantic segmentation as the research content. With the powerful feature extraction and classification capabilities of convolutional neural networks in deep learning, this paper studies the landscape classification and visualization analysis methods of high-resolution landscape remote sensing images captured under different conditions. It solves the problems of complex process and poor generalization ability of traditional landscape classification methods, and applies the classification results to the analysis of landscape pattern changes in Xindu District, obtaining the changes in landscape types and stability of landscape patterns in the region. This article demonstrates the significant research significance of integrating deep learning into landscape pattern related studies through landscape classification using remote sensing images of garden landscapes.

However, there are still some shortcomings in this article. Firstly, although the CNN-LSTM method proposed in this article has some improvement in accuracy compared to previous methods, there is still significant room for improvement, and further research is needed to improve accuracy in the future; Secondly, the currently used models are supervised learning methods, which can greatly improve the efficiency of image classification. However, a large amount of annotation work is still required in the early stage, so high-precision unsupervised methods are a direction for future research; Finally, at the current stage, the method proposed in this article only integrates deep learning into the data processing stage, but the subsequent analysis of landscape changes still uses traditional analysis methods. How to integrate deep learning into the visualization process of the entire landscape pattern change and provide greater convenience for the analysis of the entire landscape pattern change is the focus of the next research.

Author's Profile

Yanfeng Dong was born in Dangshan, Anhui, China, in 1999. He is currently studying at the College of Art, Hebei University of Science and Technology. His main research direction is design history and theory.

Mengmeng Li was born in Zhoukou, Henan, China, in 1998. She obtained a bachelor's degree from Anhui University in China. Her main research direction is landscape perception and preference, children's landscape research.

Chuan Zhao was born in Shijiazhuang, Hebei, China, in 1986. He obtained a bachelor's degree from Nanjing Normal University in China. Associate Professor of Hebei University of

Science and Technology. His main research direction is design history and theory.

References

- [1] Gu T, Luo T, Ying Z, et al. Coupled relationships between landscape pattern and ecosystem health in response to urbanization[J]. *Journal of Environmental Management*, 2024, 367: 122076.
- [2] Zhou X, Chu Z, Ji X. Changes in the land-use landscape pattern and ecological network of Xuzhou planning area[J]. *Scientific Reports*, 2024, 14(1): 8854.
- [3] Wang Q, Zhang P, Chang Y, et al. Landscape pattern evolution and ecological risk assessment of the Yellow River Basin based on optimal scale[J]. *Ecological Indicators*, 2024, 158: 111381.
- [4] Acil N, Sadler J P, Senf C, et al. Landscape patterns in stand-replacing disturbances across the world's forests[J]. *Nature Sustainability*, 2025, 8(1): 86-98.
- [5] Ocloo M D, Huang X, Fan M, et al. Study on the spatial changes in land use and landscape patterns and their effects on ecosystem services in Ghana, West Africa[J]. *Environmental Development*, 2024, 49: 100947.
- [6] Dong Y, Liu S, Pei X, et al. Identifying critical landscape patterns for simultaneous provision of multiple ecosystem services—A case study in the central district of Wuhu City, China[J]. *Ecological Indicators*, 2024, 158: 111380.
- [7] Tang J, Yu L, Zhang X, et al. A Landscape Pattern Characterization Method Based on the Natural Complex: A Case Study of Songhua River Basin, China[J]. *Chinese Geographical Science*, 2025, 35(3): 492-509.
- [8] Xu M, Matsushima H. Multi-dimensional landscape ecological risk assessment and its drivers in coastal areas[J]. *Science of The Total Environment*, 2024, 908: 168183.
- [9] Le Li C Z, Pei N, Gao B, et al. Correlation analysis of urban green landscape patterns and bird diversity based on passive acoustic monitoring technology[J]. *Biodiversity Science*, 2024, 32(10): 24296.
- [10] LYU X, GOU A, CHEN Z, et al. Landscape pattern change of marsh in the Nanmojie Wetland National Nature Reserve of Sichuan Province[J]. *Chinese Journal of Ecology*, 2024, 43(6): 1747.
- [11] Li M, Abuduwaili J, Liu W, et al. Application of geographical detector and geographically weighted regression for assessing landscape ecological risk in the Irtysh River Basin, Central Asia[J]. *Ecological Indicators*, 2024, 158: 111540.
- [12] Shen Z, Yin H, Kong F, et al. Enhancing ecological network establishment with explicit species information and spatially coordinated optimization for supporting urban landscape planning and management[J]. *Landscape and Urban Planning*, 2024, 248: 105079.

- [13] Rahimi E, Jung C. Analyzing vegetation heterogeneity trends in an urban-agricultural landscape in Iran using continuous metrics and NDVI[J]. *Land*, 2025, 14(2): 244.
- [14] Liu M, Peng J, Dong J, et al. Trade-offs of landscape connectivity between regional and interregional ecological security patterns in a junction area of Bei**g-Tian**-Hebei region[J]. *Applied Geography*, 2024, 167: 103272.
- [15] Guo Y, Ren Z, Wang C, et al. Spatiotemporal patterns of urban forest carbon sequestration capacity: Implications for urban CO₂ emission mitigation during China's rapid urbanization[J]. *Science of the Total Environment*, 2024, 912: 168781.
- [16] Li J, Hu D, Wang Y, et al. Study of identification and simulation of ecological zoning through integration of landscape ecological risk and ecosystem service value[J]. *Sustainable Cities and Society*, 2024, 107: 105442.
- [17] Huang M, Gong D, Zhang L, et al. Spatiotemporal dynamics and forecasting of ecological security pattern under the consideration of protecting habitat: A case study of the Poyang Lake ecoregion[J]. *International Journal of Digital Earth*, 2024, 17(1): 2376277.
- [18] Bai X, Yu Z, Wang B, et al. Quantifying threshold and scale response of urban air and surface temperature to surrounding landscapes under extreme heat[J]. *Building and Environment*, 2024, 247: 111029.
- [19] Zeng W, He Z, Bai W, et al. Identification of ecological security patterns of alpine wetland grasslands based on landscape ecological risks: A study in Zoigê County[J]. *Science of the Total Environment*, 2024, 928: 172302.
- [20] Gao J, Gong J, Li Y, et al. Ecological network assessment in dynamic landscapes: Multi-scenario simulation and conservation priority analysis[J]. *Land Use Policy*, 2024, 139: 107059.
- [21] Chen W, Liu H, Wang J. Construction and optimization of regional ecological security patterns based on MSPA-MCR-GA Model: A case study of Dongting Lake Basin in China[J]. *Ecological Indicators*, 2024, 165: 112169.
- [22] Li J, Huang Z, Zhu Z, et al. Coexistence Perspectives: Exploring the impact of landscape features on aesthetic and recreational values in urban parks[J]. *Ecological Indicators*, 2024, 162: 112043.
- [23] Barman S, Roy D, Chandra Sarkar B, et al. Assessment of urban growth in relation to urban sprawl using landscape metrics and Shannon's entropy model in Jalpaiguri urban agglomeration, West Bengal, India[J]. *Geocarto International*, 2024, 39(1): 2306258.
- [24] Xu Z, Wu D, Yu C, et al. Sctnet: Single-branch cnn with transformer semantic information for real-time segmentation[C]//*Proceedings of the AAAI conference on artificial intelligence*. 2024, 38(6): 6378-6386.
- [25] Dao F, Zeng Y, Qian J. Fault diagnosis of hydro-turbine via the incorporation of bayesian algorithm optimized CNN-LSTM neural network[J]. *Energy*, 2024, 290: 130326.
- [26] Yadav H, Thakkar A. NOA-LSTM: An efficient LSTM cell architecture for time series

forecasting[J]. *Expert Systems with Applications*, 2024, 238: 122333.

- [27] Tang Y, Dong P, Tang Z, et al. Vmrnn: Integrating vision mamba and lstm for efficient and accurate spatiotemporal forecasting[C]//*Proceedings of the IEEE/CVF Conference on Computer Vision and Pattern Recognition*. 2024: 5663-5673.